Hindawi
International Journal of Corrosion
Volume 2021, Article ID 6658186, 8 pages
https://doi.org/10.1155/2021/6658186

Research Article

Corrosion and Hardness Behaviour of Al/GO Nanocomposites Processed by the Ultrasonic Gravitational Stir Casting Method

S. Narayanan, G. G. Sozhamannan, K. Hemalatha, K. Velmurugan, and V. S. K. Venkatachalapathy

Department of Mechanical Engineering, Sri Manakula Vinayagar Engineering College, Pondicherry, India

Correspondence should be addressed to G. G. Sozhamannan; sozhanmech@smvec.ac.in

Received 26 October 2020; Revised 29 December 2020; Accepted 13 January 2021; Published 28 January 2021

Academic Editor: Michael J. Schütze

The objective of this work is to evaluate the corrosion behaviour of nanographene oxide reinforced aluminium (Al/GO) metal matrix composites with different immersion time periods using the immersion corrosion technique. The Al/GO composites were fabricated by the ultrasonic gravitational stir casting process. The corrosions of Al/GO were evaluated using a scanning electron microscope. The experimental results revealed that the corrosion rate decreased and weight losses increased with increasing immersion time periods. The nonimmersed Al/GO composites exhibited higher microhardness values compared to the immersed Al/GO composites.

1. Introduction

Aluminium-based metal matrix composites (AMMCs) are used mainly for manufacturing various engineering components in aerospace, automotive, defense, and other domestic applications because they have superior mechanical properties and are lightweight and have good dimensional stability. In particular, the LM 24 aluminium alloy has widely many engineering applications owing to the excellent corrosion resistance, good machinability, and excellent formability and also has hot tear resistance [1]. Therefore, LM 24 aluminium allows the usage of secondary processes such as hot extrusion, rolling, and forging [2]. The AMMCs were fabricated by the liquid state and solid state methods. The solid state method is used to fabricate a few shapes of composite components and is not suitable for the fabrication of complex-shaped components [3]. Therefore, this method is not used in many industries; however, the conventional stir casting method is widely used in many industries [4] because stir casting is a simple technique, has more flexibility, and also has more thermodynamic stability for the ceramic particles to be distributed uniformly in the matrix liquid at high temperatures producing a strong interfacial bond between the reinforcement and the matrix materials [5]. However, the conventional stir casting process is not suitable for mixing nanoparticles in the matrix liquid because of size variation, some practical issues in nanocluster formation, and inadequate wetting of nanoparticles with the matrix phase [6]. Recently, the ultrasonic cavitation assisted stir casting process replaced the conventional stir casting process, and the high intensity of ultrasonic waves breaks the cluster particles and distributes them uniformly in the matrix liquid [7–9]. Therefore, the ultrasonic stir casting technique is best suitable for the fabrication of nanocomposite materials.

In general, aluminium is a highly reactive material at high temperature [10] and has high corrosion resistance because the oxide layer present on the surface protects it from the environment. This oxide layer forms on the surface naturally when the aluminium alloy is manufactured or exposed to high temperature through the following reaction [11]: $Al + 3H_2O \longrightarrow Al(OH)_3 + 3H_2\uparrow$. The thickness of the oxide layer on the Al surface, which is stable in an aqueous medium of pH level 7.5, is about 2.5 nm. The corrosions are easily accelerated in the aluminium alloy when it is exposed to different environmental conditions, which are in contact with salt water, and when ceramic particles are added to the aluminium alloy [12]. This oxide layer dissolves when the aqueous medium level of pH is more than 9.0 or sea water. Therefore,

corrosions occur in the aluminium-based composite materials due to the addition of both micro- and nanosize ceramic particles such as SiCp, TiCp, B_4Cp, carbon nanotube (CNT), nanofiber, graphene, graphene oxide, and n-TiB_2 [13, 14]. Trowsdale et al. [15] and Han et al. recommended the Al/SiCp and Al/B_4C in 3.5 NaCl solutions to increase the susceptibility of pitting corrosion as compared to the unreinforced alloys. Abu-Warda et al. [16] reported that the addition of nano-TiB_2 did not reduce the corrosion resistance or susceptibility to pitting corrosion at the interfacial region. Recently, graphene oxide has received much attention among the nanoreinforcements due to its unique structure and outstanding mechanical properties and the presence of oxygen in graphene oxide to enhance the interfacial bond between the matrix and the reinforcement [17]. Furthermore, graphene oxide is mostly used as a coating material because of its chemical inertness and impermeability characteristics [18]. So far, investigators have mostly studied and evaluated only the mechanical behaviour of graphene oxide-based composite materials, and only a few authors concentrated on the corrosion behaviour of graphene oxide reinforced composite materials [19]. This research gap has encouraged researchers to study the corrosion behaviour of graphene oxide reinforced metal matrix composites. Different types of corrosion occur in AMMCs depending on the various manufacturing methods [20] and the physical and chemical interaction between the matrix and reinforcements at an ambient temperature level. The percentage of reinforcement plays an important role in deciding the mechanical behaviour of metal matrix composites. When increasing the percentage of nanographene oxide particles in the aluminium matrix, more nanoagglomerations are formed in the aluminium matrix. It exhibits more corrosion in the composite materials. A number of researchers have investigated the various corrosion behaviours by using different corrosion techniques. Corrosion can be divided into two categories based on the locations: one is uniform corrosion and another is localised corrosion. Uniform corrosion occurs on the surface of the composite due to the changes in environmental conditions [11], and localised corrosion mostly occurred in the matrix region and interfacial region in composite materials through chemical reactions. Localised corrosions are stress corrosion [21, 22], pitting corrosion [23], crevice corrosion, galvanic corrosion [24], and intergranular corrosion [25].

The aim of the present work is to evaluate the corrosion behaviour of Al/GO composites at different time period exposures to ambient temperature levels. The Al/GO samples were prepared by the ultrasonic stir casting method, and the corrosion behaviour in the samples was analyzed using the immersion corrosion test. Immersion corrosion testing is the most reliable and simple method for analyzing the corrosion behaviour of composite materials. The hardness strength of the corrosion samples was evaluated by microhardness testing.

2. Experimental Work

In this study, the LM 24 aluminium alloy with a density of 2.68 g/cm^3 was used as the matrix material because it has excellent casting characteristics. The 1.5 percentage nanographene particles (GO) were used as reinforcement. The average size of the graphene particles is 52 nanomicrons. The chemical composition of the LM 24 aluminium alloy is shown in Table 1. 1000 grams of LM 24 aluminium alloy was placed in a crucible and heated to 700°C at the rate of 12°C per minute. The preheated graphene oxide nanoparticles were added into the molten liquid. The liquid metal was stirred at a speed of 400 rpm using a mechanical stirrer for 10 minutes to achieve a uniform distribution of nanoparticles in the liquid metal. During this stirring process, a number of nanoclusters were formed in the liquid due to the size variation of the nanoparticles. Therefore, the mechanical stirrer was removed from the molten metal, and the ultrasonic horn was inserted in the liquid metal to one-third the height of the liquid for the purpose of inducing ultrasonic waves throughout the liquid metal. The power and frequency of the ultrasonic transducer device were 2 kW and 20 kHz, and the processing temperature was maintained at 700°C. The transducer horn produced ultrasonic waves in the liquid metal. These generated waves spread throughout the liquid and produced mechanical vibrations. These vibrations served to break up the cluster of nano-GO particles and distribute them uniformly in the liquid matrix. The composite slurry was poured into the preheated mild steel die and allowed to solidify. The casting sample of the Al/GO composite is shown in Figure 1. The size of the Al/GO composite casting is $130 \times 60 \times 15\,\text{mm}^3$. The corrosion test was carried out using a simple immersion test. The Al/GO composite samples were totally immersed in the 3.5% NaCl electrolyte for different periods of time, such as 24 hrs, 48 hrs, and 72 hrs. The corrosion samples were prepared from the composite materials and polished by a 500 grit sheet. The size of the corrosion sample was 10 mm length, 10 mm breadth, and 5 mm thickness. The weight of the Al/GO composites was measured using a weighing machine. The accuracy of the weighting machine is 0.001 grams. The specimens were immersed in 250 ml of 3.5% NaCl electrolyte solution. After completing the time period, the specimens were taken out from the solution and cleaned using acetone, and then, the mass losses were calculated. Figure 2 shows the corrosion and noncorrosion of the Al/GO composite. The structural changes on the sample surface were examined by a scanning electron microscope. The corroded surface strength was measured by the microhardness test.

3. Results and Discussion

3.1. Structural Analysis. The SEM micrographs of the Al/nanographene oxide composites are shown in Figure 3. The nanographene oxide particles were distributed almost uniformly in the Al matrix material. The uniformity in the distribution of the particles and the strong interfacial bonds were achieved using the ultrasonic stir casting method under optimum fabrication conditions. The corroded surfaces of the Al/GO composite samples are shown in Figure 4. The SEM micrograph clearly shows that the surface morphologies were damaged by dissolution of the aluminium layer in the NaCl solution under the immersion

Table 1: Chemical composition of LM 24 aluminium alloy.

Alloy	Cu	Mg	Si	Fe	Mn	Ni	Zn	Pb	Sn	Ti	Al
Percentage of composition	3.0-4.0	3 max.	7.5-9.5	1.3	0.5	0.5	3	0.3	0.2	0.2	Remainder

Figure 1: Casting sample of Al/GO composite.

conditions. Figure 5 shows that the surface damages were observed due to the prolonged contact period. Within the initial immersion period, more surface damages were not observed, and it is shown in Figure 4. During the immersion periods, the presence of carbon in the nanographene oxide reacts with the aluminium to form aluminium carbide at the interfacial region. Smith et al. [26] reported that nanographene oxide has a carbon element in the hexagonal structure. The EDS analysis was carried out in the interfacial region using a line scanning option method. This analysis confirmed the presence of the carbon element in the interfacial region, as shown in Figure 6. The aluminium carbide reaction takes place in the following manner: $Al_2 + 3C \longrightarrow Al_2C_3$. The presence of intermetallic elements of alumina carbide (Al_4C_3) which forms at the interfacial region initiated localised corrosion in and around the reinforcement. It is expected that there will be increased susceptibility to corrosion at the interfacial region between the Al matrix and the nanographene oxide reinforcement. Under prolonged immersion periods, the intermetallic elements were diluted in the NaCl solution and initiated the debonding between the Al matrix and the graphene oxide particles. The interfacial microcracks formed on the surface and interfacial region as shown in Figure 7. This is a favourable mechanism for debonding and corrosion formation in the A/GO composites.

3.2. Weight Loss and Water Absorption of Al/GO Composites. The weight losses in the Al/GO composite samples were measured after completion of the immersion period using a high accuracy weighing machine. The weight losses of the Al alloy and Al/GO samples are shown in Figure 8. The Al/GO composites have more weight losses than the Al alloy due to the dilution of intermetallic compounds at the interfacial region and surface deterioration in the composites. The weight measurement revealed that the weight losses increased with increases in the time period due to the surface corrosion, dissolving of the oxide layer, and pitting corrosion in the composite materials.

The NaCl absorptions were calculated according to the following equation [27]: NaCl absorption (%) = (Wt.of wet sample − Wt.of dry sample)/(Weight of dry sample) × 100. Figure 9 shows the absorption curve of the immersion time periods. The NaCl absorption in the composites occurred by a diffusion process. The NaCl is diffused in the matrix and interfacial region of the composites through surface microcracks. The surface microcracks were formed during the fabrication of the composites and covered by an oxide layer [28]. The presence of microcracks in the Al/GO sample is shown in Figure 7. The surface microcracks were observed due to the dissolving of oxide layers when in contact with the NaCl solution. Therefore, the NaCl absorption rate increased with the increased immersion time period.

3.3. Corrosion Behaviours of Al/GO Composites. The corrosion rate of the composite was calculated following the equation [29]: corrosion rate (mm/year) = $87.6W/DAT$, where W is the weight loss of the exposed samples in grams, D is the density of specimen in g/cm^3, A is the area of the exposed samples in cm^2, and T is exposure time in hours. The corrosion rate of the Al/GO composites is shown in Figure 10. The corrosion rates of both Al alloy and Al/GO composites showed similar trends, but the Al alloy exhibited a lower corrosion rate compared to the Al/GO samples due to the absence of nanoreinforcements in the matrix. The corrosion rate was high in the initial period of immersion due to the adsorption of chloride ions on the surface of the Al/GO composites and as it was the first stage of localised corrosion attack on the samples. The localised corrosion formation and surface damage are shown in Figures 4 and 5. The previous investigator Falcon et al. [30] reported that the surface corrosion and pitting corrosion in the composite materials take place through the following steps: (a) adsorption and diffusion of chloride ions on the oxide surface, (ii) formation of hydroxychloride aluminium salts, and (iii) dissolution of the oxide. When the immersion period was increased, the chloride solution diffused in the composite material through the existing surface microcracks. The presence of surface microcracks on the composite sample is shown in Figure 7. A minimum amount of the chloride solution was diffused in the interfacial region and other boundary areas in the Al matrix to initiate the corrosion inside the composites. Therefore, the corrosion rate decreased with the increase in the immersion time periods. The corrosion pits observed in the composite sample were shown in Figure 11. The corrosion pits appear cup-shaped, hemispherical, flat-walled, or sometimes irregular-shaped depending upon the preferential corrosion area, adsorption and diffusion of the chloride ions, and immersion periods [31]. The irregular shapes of the corrosion pits were found at the interfacial region between the Al matrix and the GO particles. It is shown in Figure 11. These corrosion pits are weakly passivized or thermodynamically unstable. Therefore, the interfacial region can serve as nucleation sites for pit formation. Finally, the experimental

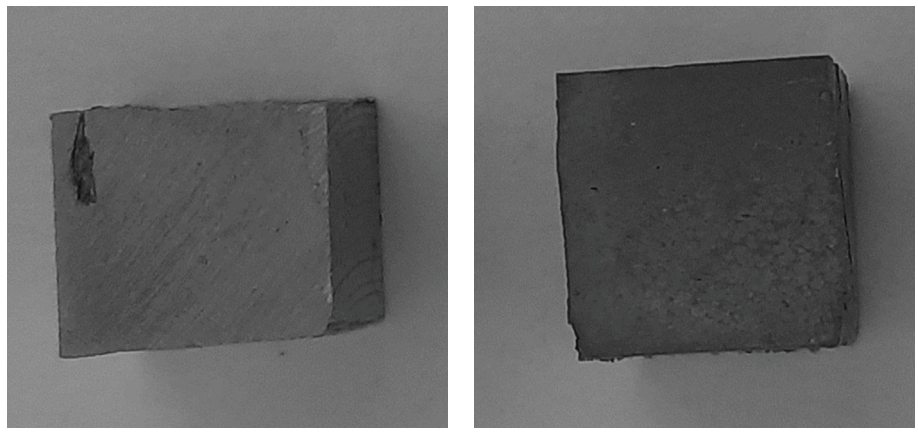

(a) (b)

Figure 2: (a) Al/GO composite noncorrosion sample; (b) Al/GO composite corrosion sample.

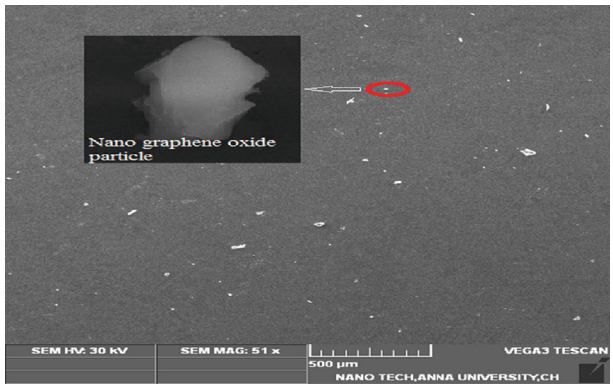

Figure 3: Nanoparticle distribution in Al/GO composite.

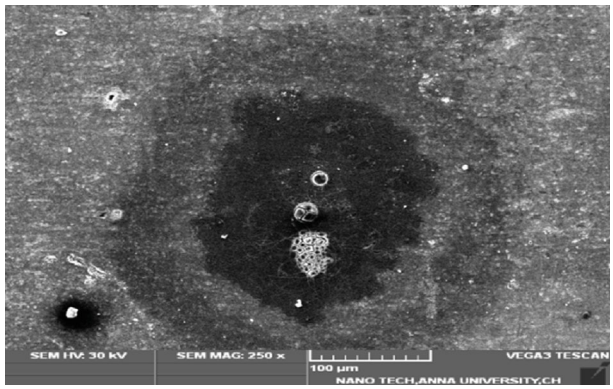

Figure 4: Corroded surfaces of Al/GO composite.

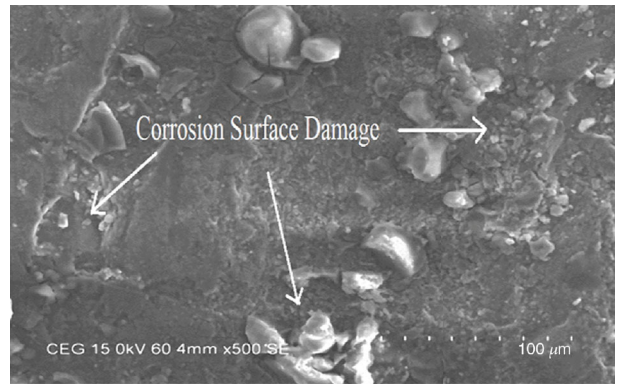

Figure 5: Corrosion surface damages of the Al/GO composite.

results revealed that the corrosion rates depend mainly on the immersion period, chloride ions, interfacial region, and surface conditions of the composite materials.

3.4. Effect of Hardness Strength on Al/GO Composites. This analysis is used to study the effect of the hardness strength of both the noncorroded and corroded surfaces on the composite samples and the interfacial region between the Al matrix and GO nanoparticles. The microhardness measurement experiments were conducted before and after the corrosion analysis of the different periods of immersion tests. The microhardness values were measured on the specimens at different points at constant distance intervals. Figure 12 shows the different hardness variations depending on the surface morphology conditions and the distribution of nanographene oxide particles in the Al matrix. However, a comparison of the different samples with different immersion periods shows that the nonimmersed samples show higher microhardness values when compared to the corroded samples due to the presence of the oxide layer on the surface and the uniformity in the distribution of the nanoparticles. The nanoparticles bonded well with the Al matrix, as shown in Figure 1. The deformation of the Al matrix was restricted by the presence of nano-GO particles during the loading conditions. Therefore, the nonimmersed samples provided higher hardness strength. The initial immersion periods (24 hrs.), the surface damage, and surface corrosion occurred due to the adsorption of chloride ions in the Al/GO samples. Therefore, the microhardness gradually decreases in these samples compared to the nonimmersion sample. When the immersion periods were increased from 24 hrs. to 72 hrs., the chloride solutions diffused in the Al matrix and the interfacial region between the Al matrix and GO particles through the preexisting

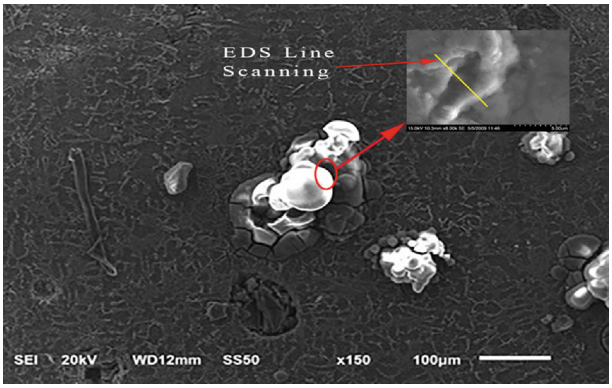

(a)

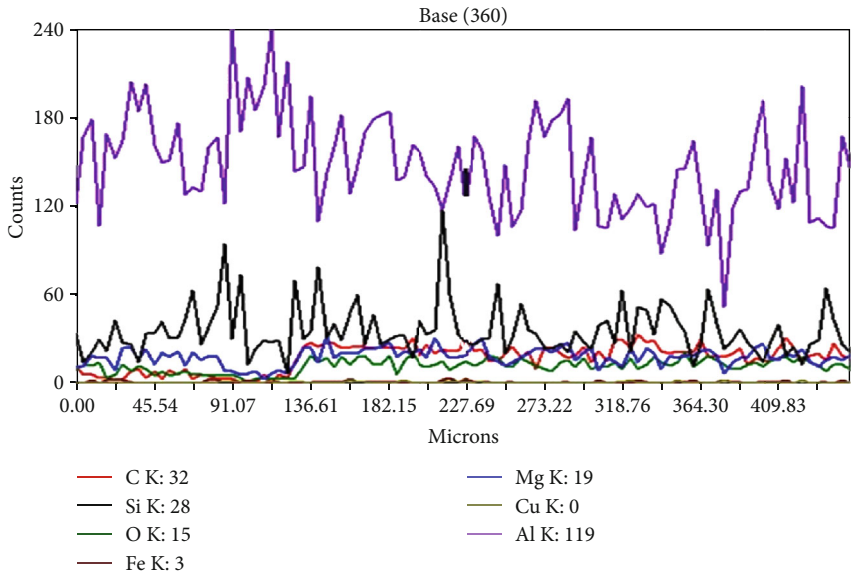

(b)

Figure 6: (a) SEM image of Al/GO composite; (b) EDS analysis.

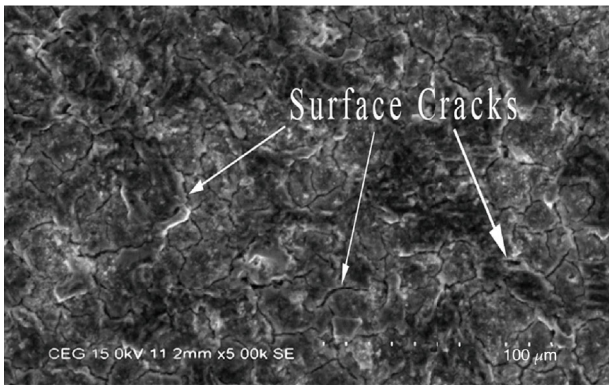

Figure 7: Surface microcracks of Al/GO composite.

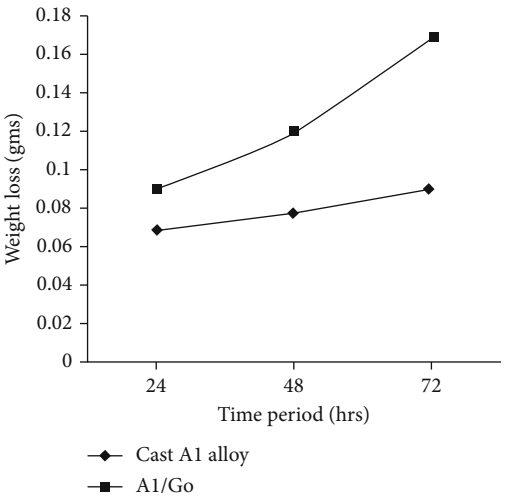

Figure 8: Weight loss of the Al/GO corrosion samples.

microcracks. During prolonged immersion periods, the aluminium salts became diluted and created corrosion pits in the Al matrix region as shown in Figure 9. When an indenter load was applied on the Al/GO specimens, the plastic deformation was relatively large and the movement

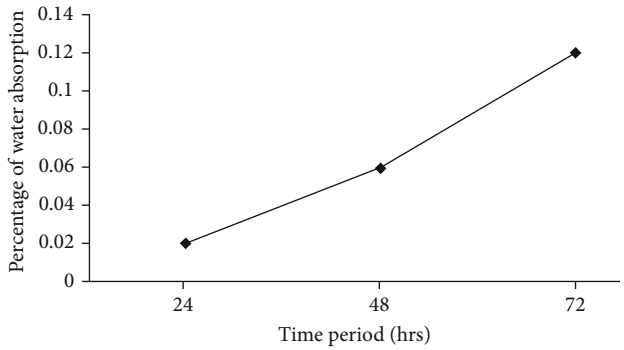

Figure 9: Water absorption of Al/GO samples.

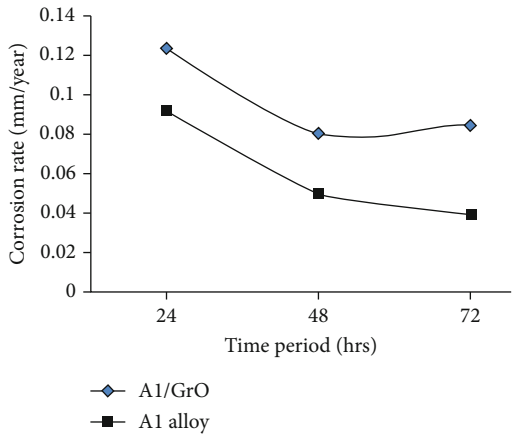

Figure 10: Corrosion rates of the Al/GO composites.

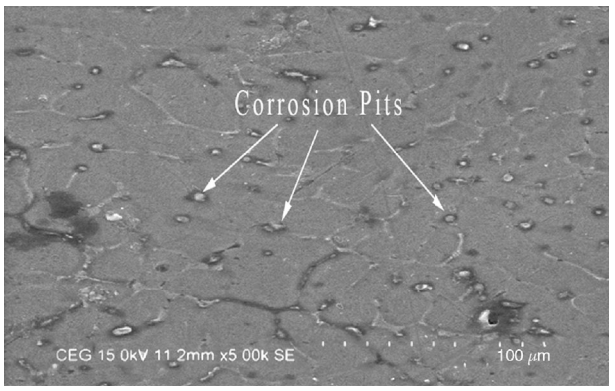

Figure 11: Corrosion pits of the Al/GO composite.

of Al matrix dislocations became much easier due to the presence of corrosion pits in the Al matrix region. The microhardness analysis revealed that the hardness strength of the composite materials depends on the surface morphologies and the interfacial bond between the matrix and the reinforcement.

3.5. Tensile Properties of Al/GO Composites. The property of Al/GO composites depends mainly on the distribution of the nanoparticles in the matrix. It is necessary to understand the particle distribution in the matrix in order to correlate the

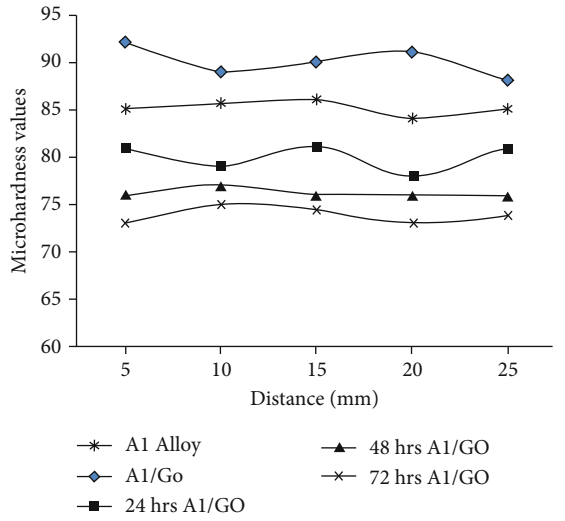

Figure 12: Microhardness values of the Al/GO composites.

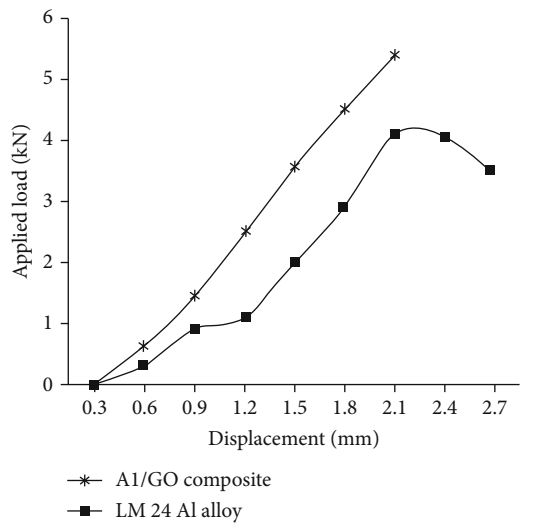

Figure 13: Tensile cure for Al/GO composites.

properties of the PRMMCs. The tensile test was conducted on a flat-shaped specimen, performed according to the ASTM standard (E-8 model) test methods.

Figure 13 shows the variation in the ultimate tensile strength Al/GO composites. The Al/GO composites exhibit more tensile strength compared to the aluminium alloy. The overall strength of the composites is influenced by the distribution of the graphene nanoparticles in the Al matrix.

4. Conclusions

The corrosion behaviour of Al/GO composites was investigated by using immersion for different periods. The following results can be inferred from this experimental work:

(1) From the SEM micrograph analysis, the nanographene oxide particles were seen distributed uniformly in the Al matrix (using ultrasonic stir casting method)

(2) The Al/GO composites experience more surface deterioration due to the corrosion on the surface and adsorption of NaCl ions on the surface. A number of corrosion pits were observed in the Al matrix region and the interfacial region

(3) The weight losses increased with the increase in immersion periods, and the intermetallic compound, and aluminium oxide layer dissolved in the 3.5% of NaCl solution

(4) 3.5% of NaCl solution was diffused in the composite material through the surface cracks. The water absorption rate percentage increased with the increase in immersion time periods

(5) The Al alloy exhibited less corrosion compared to the Al/GO composites. The corrosion rate in the alloy decreased with the increase in immersion periods. The immersion test revealed that the corrosions on the surface and interfacial regions in the composites depend mainly on adsorption and the diffusion of the NaCl solution in preferential corrosion areas and time periods

(6) The microhardness test results exhibited that the non-Al/GO composite samples exhibited more hardness in strength compared to the corroded Al/GO samples. The corroded surfaces have more surface damage and corrosion pits in the interfacial region. Hence, it produced less hardness in strength

(7) The tensile test revealed that the nanographene oxide reinforced composite provided more strength compared to the unreinforced aluminium alloy. The presence of nano-GO particles improved the mechanical strength of aluminium-based composites

Data Availability

No data used to support the study.

Conflicts of Interest

The authors declare that they have no conflicts of interest.

References

[1] P. Vijian and V. P. Arunachalam, "Modelling and multi objective optimization of LM24 aluminium alloy squeeze cast process parameters using genetic algorithm," *Journal of Materials Processing Technology*, vol. 186, no. 1-3, pp. 82–86, 2007.

[2] C. S. Ramesh and M. Safiulla, "Wear behavior of hot extruded Al6061 based composites," *Wear*, vol. 263, no. 1-6, pp. 629–635, 2007.

[3] G. B. Jang, M. D. Hur, and S. S. Kang, "A study on the development of a substitution process by powder metallurgy in automobile parts," *Journal of Materials Processing Technology*, vol. 100, no. 1-3, pp. 110–115, 2000.

[4] S. B. Prabu, L. Karunamoorthy, S. Kathiresan, and B. Mohan, "Influence of stirring speed and stirring time on distribution of particles in cast metal matrix composite," *Journal of Materials Processing Technology*, vol. 171, no. 2, pp. 268–273, 2006.

[5] J. Hashim, L. Looney, and M. S. J. Hashmi, "Metal matrix composites: production by the stir casting method," *Journal of Materials Processing Technology*, vol. 92-93, pp. 1–7, 1999.

[6] J. Hashim, L. Looney, and M. S. J. Hashmi, "Particle distribution in cast metal matrix composites–part I," *Journal of Materials Processing Technology*, vol. 123, no. 2, pp. 251–257, 2002.

[7] A. H. Idrisi and A.-H. I. Mourad, "Conventional stir casting versus ultrasonic assisted stir casting process: mechanical and physical characteristics of AMCs," *Journal of Alloys and Compounds*, vol. 805, pp. 502–508, 2019.

[8] M. Malaki, W. Xu, K. A. Kasar et al., "Advanced metal matrix nanocomposites," *Metals*, vol. 9, no. 3, p. 330, 2019.

[9] D. K. Koli, G. Agnihotri, and R. Purohit, "Influence of ultrasonic assisted stir casting on mechanical properties of Al6061-nano Al2O3 composites," *Materials Today: Proceedings*, vol. 2, no. 4-5, pp. 3017–3026, 2015.

[10] B. Bobic, S. Mitrovic, M. Babic, and J. Bobic, "Corrosion of aluminium and zinc-aluminium alloys based metal-matrix composites," *Tribology in Industry*, vol. 31, pp. 44–54, 2009.

[11] P. S. S. Ratna Kumar, S. J. Alexis, and D. S. R. Smart, "Uniform Corrosion Behavior of AA7075 with Nanoclay," *Materials Today: Proceedings*, vol. 4, no. 8, pp. 9013–9019, 2017.

[12] Z. Szklarska-Smialowska, "Pitting corrosion of aluminum," *Corrosion Science*, vol. 41, no. 9, pp. 1743–1767, 1999.

[13] M. Albiter, J. B. Contreras, M. Salazar, and J. G. Gonzalez-Rodriguez, "Corrosion behaviour of aluminium metal matrix composites reinforced with TiC processed by pressureless melt infiltration," *Journal of Applied Electrochemistry*, vol. 36, no. 3, pp. 303–308, 2006.

[14] H. Asgharzadeh and M. Sedigh, "Synthesis and mechanical properties of Al matrix composites reinforced with few-layer graphene and graphene oxide," *Journal of Alloys and Compounds*, vol. 728, pp. 47–62, 2017.

[15] A. J. Trowsdale, B. Noble, S. J. Harris, I. S. R. Gibbins, G. E. Thompson, and G. C. Wood, "The influence of silicon carbide reinforcement on the pitting behaviour of aluminium," *Corrosion Science*, vol. 38, no. 2, pp. 177–191, 1996.

[16] N. Abu-Warda, M. D. Lopez, M. D. Escalera-Rodriguez, E. Otero, and M. V. Utrilla, "Corrosion behavior of mechanically alloyed A6005 aluminum alloy composite reinforced with TiB2nanoparticles," *Materials and Corrosion*, vol. 71, no. 3, pp. 382–391, 2020.

[17] M. Hedayatian, K. Vahedi, A. Nezamabadi, and A. Momeni, "Microstructural and mechanical behavior of Al6061-graphene oxide nanocomposites," *Metals and Materials International*, vol. 26, no. 6, pp. 760–772, 2020.

[18] M. Y. Rekha, A. Kamboj, and C. Srivastava, "Electrochemical behaviour of SnZn-graphene oxide composite coatings," *Thin Solid Films*, vol. 636, pp. 593–601, 2017.

[19] J. Li, H. Zhang, F. Sun, H. Zhou, L. Zhao, and Y. Song, "The multiscale effects of graphene oxide on the corrosion resistance properties of waterborne alkyd resin coatings," *Journal of Materials Research*, vol. 34, no. 6, pp. 950–958, 2019.

[20] F. Walsh, G. Ottewill, and D. Barker, "Corrosion and protection of metals: II. Types of corrosion and protection methods," *Transactions of the IMF*, vol. 71, pp. 117–120, 2017.

[21] L. S. Kuburi, M. Dauda, S. A. Yaro, and M. Abdulwahab, "Study of the microstructure and stress corrosion cracking (SCC) resistance of marine grade aluminium matrix

composite," *Mechanics and Mechanical Engineering*, vol. 21, pp. 833–841, 2017.

[22] Z. Yin, F. Liu, D. Song, S. He, J. Lin, and F. Yu, "Stress corrosion cracking of a forged Mg-Al-Zn alloy with different surface conditions," *Journal of Chemistry*, vol. 2018, Article ID 4262860, 8 pages, 2018.

[23] I. Gurrappa and V. V. Bhanu Prasad, "Corrosion characteristics of aluminium based metal matrix composites," *Materials Science and Technology*, vol. 22, pp. 115–124, 2013.

[24] H. M. Zakaria, "Microstructural and corrosion behavior of Al/SiC metal matrix composites," *Ain Shams Engineering Journal*, vol. 5, no. 3, pp. 831–838, 2014.

[25] J. F. McIntyre and T. S. Dow, "Intergranular corrosion behavior of aluminum alloys exposed to artificial seawater in the presence of nitrate anion," *Corrosion*, vol. 48, no. 4, pp. 309–319, 1992.

[26] A. T. Smith, A. M. LaChance, S. Zeng, B. Liu, and L. Sun, "Synthesis, properties, and applications of graphene oxide/reduced graphene oxide and their nanocomposites," *Nano Materials Science*, vol. 1, no. 1, pp. 31–47, 2019.

[27] M. Hussain and K. Niihara, "Control of water absorption and its effect on interlaminar shear strength of CFRC with Al_2O_3 dispersion," *Materials Science and Engineering*, vol. 272, no. 2, pp. 264–268, 1999.

[28] B. Bobić, J. Bajat, I. Bobić, and B. Jegdić, "Corrosion influence on surface appearance and microstructure of compo cast ZA27/SiC_p composites in sodium chloride solution," *Transactions of Nonferrous Metals Society of China*, vol. 26, no. 6, pp. 1512–1521, 2016.

[29] R. A. Freeman and D. C. Silverman, "Technical note: error propagation in coupon immersion tests," *Corrosion*, vol. 48, no. 6, pp. 463–466, 1992.

[30] L. A. Falcon, E. B. Bedolla, J. Lemus, C. Leon, I. Rosales, and J. G. Gonzalez-Rodriguez, "Corrosion behavior of Mg-Al/TiC composites in NaCl solution," *International Journal of Corrosion*, vol. 2011, Article ID 896845, 7 pages, 2011.

[31] K. V. Akpanyung and R. T. Loto, "Pitting corrosion evaluation: a review," *Journal of Physics: Conference Series*, vol. 1378, article 022088, 2019.